IEEE Control Systems Letters paper presented at
2023 62nd IEEE Conference on Decision and Control (CDC)
December 13-15, 2023. Marina Bay Sands, Singapore

A Novel Viral Infection Model to Guide Optimal Mpox Treatment

Maarten de Jong[a], Francesca Calà Campana[b], Pengfei Li[c], Qiuwei Pan[c], and Giulia Giordano[b]

***Abstract*— In 2022, worldwide mpox outbreaks have called attention to mpox virus infection and treatment opportunities using the drugs *cidofovir* and *tecovirimat*, which target different stages of in-host viral proliferation, respectively production and shedding. We propose a new model of in-host viral infection dynamics that distinguishes between the two stages, so as to explore the distinct effects of the two drugs, and we analyse the model properties and behaviour. Reducing the model order via timescale separation is shown to lead to the classical target-cell limited model, with a lumped viral proliferation rate depending on both production and shedding. We explicitly introduce the effect of the two drugs and we exemplify how to formulate and solve an optimal control problem that leverages the model dynamics to schedule optimal combined treatments.**

I. Introduction: Mpox Dynamics and Treatment

Since its discovery in 1970, the monkeypox, or mpox, virus has been mostly confined to African tropical regions. In 2022, mpox outbreaks were registered in non-endemic countries in Europe and America [1]–[3]. As any virus, mpox proliferates in the host by infecting host cells and turning them into virus-producing (productive) cells. Antiviral agents *cidofovir* and *tecovirimat* inhibit mpox proliferation. *Cidofovir* inhibits viral production: it binds to viral DNA polymerase, thereby inhibiting a crucial step in the viral assembly inside a productive cell [4], [5]. *Tecovirimat* inhibits viral shedding: it curbs the production of enveloped extracellular virus by inhibiting envelope protein p37; although non-enveloped mature internal viruses can also leave the host cell at cell death, enveloped virus is thought to be the major contributor to cell-to-cell transmission [6]–[8].

Mathematical models have been successfully proposed to describe the in-host evolution of infectious diseases and plan the optimal treatment of viral infections, including HIV and COVID-19 [9]–[15]. The classic *target-cell limited model* [16], [17] of viral infection describes the interplay among three populations (uninfected target cells; infected productive cells; virus) and lumps the production of new virus within infected cells and its subsequent shedding into a single process. However, this prevents the exploration of the distinct effects of *cidofovir* and *tecovirimat* on mpox infection.

The main contribution of this paper is to propose and analyse a new model structure that explicitly shows the effect of reducing the viral production rate p and shedding rate η.

- Our new model (Section II) considers five populations: uninfected target cells, C_U; latent cells, C_L, that are infected but not yet producing virus; infected productive cells, C_P; intracellular virus V_I; enveloped extracellular virus, V_E, able to infect cells. We show that reducing the model via timescale separation techniques yields a target-cell limited model with a lumped constant for extracellular virus production that depends on both p and η; yet, we consider the full model to capture the specific effect of each drug and exemplify how therapies can be planned accordingly.
- We thoroughly analyse the model behaviour, characterise the disease-free equilibrium set and assess its stability, also in relation to the reproduction number (Section III).
- Considering mpox dynamics when *cidofovir* and *tecovirimat* can be infused, and possible parameter values from the literature, we formulate and solve an optimal control problem (Section IV), to demonstrate how our model could be used to plan antiviral treatments that optimally combine both drugs.

II. Mpox Virus Infection Model

We consider in-host mpox infection dynamics involving five state variables associated with the populations of: uninfected cells, C_U [N]; latent cells, C_L [N]; productive cells, C_P [N]; intracellular virus, V_I [N]; infective extracellular virus, V_E [N], where [N] is the number of cells or virus particles in a given volume. The infection cycle is visualized in Fig. 1, and the dynamics are described by the system

$$\dot{C}_U(t) = -\beta C_U(t) V_E(t) \tag{1a}$$
$$\dot{C}_L(t) = \beta C_U(t) V_E(t) - \gamma C_L(t) \tag{1b}$$
$$\dot{C}_P(t) = \gamma C_L(t) - \delta C_P(t) \tag{1c}$$
$$\dot{V}_I(t) = p C_P(t) - \eta V_I(t) - f_\delta(C_P) \tag{1d}$$
$$\dot{V}_E(t) = \eta V_I(t) - c V_E(t) \tag{1e}$$

where all the parameters are positive: β $\left[(\text{t N})^{-1}\right]$ represents the infection coefficient; γ $\left[\text{t}^{-1}\right]$ is the rate constant of progression of an infected cell from latent to productive; δ $\left[\text{t}^{-1}\right]$ is the death rate constant of productive cells; p $\left[\text{t}^{-1}\right]$ is the viral production rate constant; η $\left[\text{t}^{-1}\right]$ is the viral shedding rate constant; c $\left[\text{t}^{-1}\right]$ is the clearance rate constant of extracellular virus. Vital dynamics of uninfected cells, death of latent cells and clearance dynamics of intracellular virus are assumed to be negligible over the considered time scale. The dynamics of V_I involve production, shedding, and viral loss occurring due to productive cell death events at a rate $f_\delta(C_P) \geq 0$. Virus lost in such events is not enveloped, thus it does not add to the external virus population [8]. The reaction of the immune system is implicitly accounted

The work of Maarten de Jong was supported by NWO through the research project SYNERGIA under grant n. 17626. The work of Giulia Giordano was supported by the European Union through the research project ERC INSPIRE under grant n. 101076926.

[a] Delft Center for Systems and Control, Delft University of Technology, The Netherlands. m.n.dejong@tudelft.nl

[b] Department of Industrial Engineering, University of Trento, Italy. {f.calacampana;giulia.giordano}@unitn.it

[c] Department of Gastroenterology and Hepatology, Erasmus MC – University Medical Center, Rotterdam, The Netherlands.

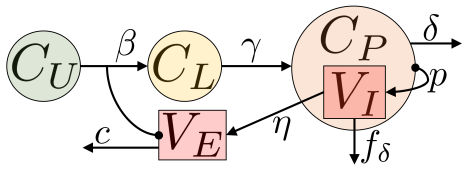

Fig. 1: Virus reproduction cycle corresponding to system (1). Uninfected cells C_U are infected by external virus V_E with rate constant β. The resulting latent cells C_L are transformed with rate constant γ into virus producing cells C_P, which produce internal virus with rate constant p and die with rate constant δ. Internal virus V_I is shed with rate constant η, thus producing external virus, which is cleared with rate constant c. Internal virus is also lost, due to the death of productive cells, at rate f_δ.

for by the parameters: the immune response reduces β and increases δ and c. The two drugs *cidofovir* and *tecovirimat* would reduce p and η, respectively.

To find an expression for the reduction of intracellular virus caused by productive cell death, we consider the virus population inside a single productive cell, $V_{I,C}(t)$. Experiments on isolated host cells have shown that, after the latent period, internal virus particles are produced at a constant rate p [18] and are then shed from the cell through the process of extracellular enveloped virus formation, which requires membrane protein p37 [8], [19]. The shedding process is modelled as proportional to the amount of internal virus, with rate constant η. Therefore, the internal virus population evolves as:

$$\dot{V}_{I,C}(t) = p - \eta V_{I,C}(t). \tag{2}$$

The average lifespan of a productive cell is δ^{-1}. Given the solution $V_{I,C}(t) = \frac{p}{\eta}\left(1 - \mathrm{e}^{-\eta t}\right)$ to (2), the average number of intracellular virus copies lost due to one cell death is $V_{I,C}(\delta^{-1}) = \frac{p}{\eta}\left(1 - \mathrm{e}^{-\frac{\eta}{\delta}}\right)$, corresponding to the intracellular virus population in the average productive cell at the end of its life. Multiplying this term by the death rate δC_P for all productive cells yields $f_\delta(C_P) = \frac{p}{\eta}\left(1 - \mathrm{e}^{-\frac{\eta}{\delta}}\right)\delta C_P$. Hence,

$$\dot{V}_I(t) = pC_P(t) - \eta V_I(t) - \frac{\delta}{\eta}\left(1 - \mathrm{e}^{-\frac{\eta}{\delta}}\right) pC_P(t). \tag{3}$$

By defining

$$p_r \doteq \psi\left(\frac{\eta}{\delta}\right) p, \;\text{ with }\; \psi\left(\frac{\eta}{\delta}\right) \doteq \left[1 - \frac{\delta}{\eta}\left(1 - \mathrm{e}^{-\frac{\eta}{\delta}}\right)\right], \tag{4}$$

we can rewrite (3) so that the full model, with state $x(t) = [C_U(t)\, C_L(t)\, C_P(t)\, V_I(t)\, V_E(t)]^\top$, becomes

$$\dot{C}_U(t) = -\beta C_U(t) V_E(t) \tag{5a}$$
$$\dot{C}_L(t) = \beta C_U(t) V_E(t) - \gamma C_L(t) \tag{5b}$$
$$\dot{C}_P(t) = \gamma C_L(t) - \delta C_P(t) \tag{5c}$$
$$\dot{V}_I(t) = p_r C_P(t) - \eta V_I(t) \tag{5d}$$
$$\dot{V}_E(t) = \eta V_I(t) - c V_E(t) \tag{5e}$$

The state variables, associated with population densities, cannot become negative, or arbitrarily large.

Proposition 1 (Positivity and boundedness)**.** *System* (5) *is positive (*$\forall i,\ x_i(t) \geq 0$ *for all* $t \geq t_0$ *if* $x_i(t_0) \geq 0$*) and bounded (for any initial state with* $x_i(t_0) \geq 0\ \forall i$*, there exist positive constants* k_i *such that* $x_i(t) \leq k_i$ *for all* $t \geq t_0$*).*

Proof. All the system parameters are positive, including p_r. In fact, since $\frac{\eta}{\delta} > 0$, also $\psi(\frac{\eta}{\delta})$ is positive: it is monotonically increasing, with $\lim_{\frac{\eta}{\delta}\to 0} \psi\left(\frac{\eta}{\delta}\right) = 0$ and $\lim_{\frac{\eta}{\delta}\to\infty} \psi\left(\frac{\eta}{\delta}\right) = 1$. Then, the state variables cannot become negative, because for all i, when $x_i = 0$, $\dot{x}_i \geq 0$.

Since $\dot{C}_U + \dot{C}_L + \dot{C}_P \leq 0$, it is $C_U(t) + C_L(t) + C_P(t) \leq \kappa \doteq C_U(t_0) + C_L(t_0) + C_P(t_0)\ \forall\ t \geq t_0$. Variables C_U, C_L and C_P are individually upper bounded by κ, because they cannot be negative. Then, $V_I(t) \leq \frac{\kappa p_r}{\eta}$ and $V_E(t) \leq \frac{\kappa p_r}{c}$ $\forall t \geq t_0$. Boundedness of the trajectories is ensured. □

We can reduce the model by exploiting two time-scale separation arguments. If cells start producing virus very soon after infection, the dynamics of the latent cell population C_L can be neglected and $\gamma C_L = \beta C_U V_E$. Also, if the intracellular virus population is assumed to be in a quasi-steady state, then $V_I = \frac{p}{\eta}\psi\left(\frac{\eta}{\delta}\right) C_P$ can be plugged into the equation of $\dot{V}_E$. The resulting reduced-order model with state $x(t) = [C_U(t)\, C_P(t)\, V_E(t)]^\top$

$$\dot{C}_U(t) = -\beta C_U(t) V_E(t) \tag{6a}$$
$$\dot{C}_P(t) = \beta C_U(t) V_E(t) - \delta C_P(t) \tag{6b}$$
$$\dot{V}_E(t) = p_r C_P(t) - c V_E(t) \tag{6c}$$

has the same form as the classical target-cell limited model, but the production rate p_r of extracellular virus depends on both the shedding rate η and the production rate p, as in (4).

To be able to capture the specificity of each drug action at best, henceforth we focus on the complete model (5).

III. Analysis of the In-Host Infection Dynamics

We provide a qualitative analysis of the dynamics of the complete system (5). Similar results are known to hold for the target-cell limited model, as proven e.g. in [9].

A. Equilibria, reproduction number, critical cell number

As shown in Proposition 1, system (5) is positive, since $\mathbb{R}^5_{\geq 0}$ is an invariant set for the system, and its trajectories are ultimately bounded in the compact and convex set $\mathcal{X}_\infty = \{x \in \mathbb{R}^5 \colon 0 \leq x \leq x^{max}\}$. This ensures the existence of a steady state in $\mathcal{X}_\infty$ [20], [21]. Only two types of steady states are possible: the trivial equilibrium, where all state variables are zero; and the disease-free equilibrium, where only C_U has a strictly positive value, while all other variables are zero. The equilibrium set is therefore

$$\mathcal{X}_{eq} = \{x \in \mathbb{R}^5 \colon C_U \geq 0,\, C_L = C_P = V_I = V_E = 0\}. \tag{7}$$

We consider the set of meaningful initial conditions

$$\mathcal{X} = \{x \in \mathbb{R}^5_{\geq 0} \colon C_U > 0,\, V_E > 0\}. \tag{8}$$

If the infection occurs at time t_0, it leads to a discontinuity in $V_E(t)$: when $t < t_0$, all variables are zero apart from the strictly positive C_U (healthy state); for $t = t_0$, all state variables are zero apart from the strictly positive C_U and V_E.

The infection progression can be related to the in-host basic reproduction number $\mathcal{R}_0$ (defined as the number of host cells infected by a single infected cell when a small

initial viral load targets a population of $C_{U,0} > 0$ uninfected cells), which can be computed as the spectral radius of the next-generation matrix [22], [23]. For system (5), we have

$$\mathcal{R}_0 = \frac{p_r \beta}{\delta c} C_{U,0}. \tag{9}$$

The critical number $\mathcal{C}_U^*$ of uninfected cells, defined as the value of $C_{U,0}$ that solves (9) for $\mathcal{R}_0 = 1$, is

$$\mathcal{C}_U^* = \frac{\delta c}{p_r \beta}. \tag{10}$$

Note that $C_U(t) < \mathcal{C}_U^*$ if and only if $\mathcal{R}(t) \doteq \frac{p_r \beta}{\delta c} C_U(t) < 1$.

To perform a local stability analysis, we evaluate the system Jacobian matrix at the equilibrium $\bar{x} = [\bar{C}_U \, 0 \, 0 \, 0 \, 0]$:

$$J_{\bar{x}} = \begin{bmatrix} 0 & 0 & 0 & 0 & -\beta \bar{C}_U \\ 0 & -\gamma & 0 & 0 & \beta \bar{C}_U \\ 0 & \gamma & -\delta & 0 & 0 \\ 0 & 0 & p_r & -\eta & 0 \\ 0 & 0 & 0 & \eta & -c \end{bmatrix} = \left[\begin{array}{c|c} 0 & \mathbf{c} \\ \hline \mathbf{0} & \mathbf{A} \end{array}\right]. \tag{11}$$

The block-triangular matrix $J_{\bar{x}}$ is singular and its spectrum is completed by the eigenvalues of $\mathbf{A}$, whose characteristic polynomial has all positive coefficients apart from the constant term $a_0 = \gamma\eta(\delta c - p_r \beta \bar{C}_U)$. The Routh-Hurwitz table reveals that the disease-free equilibrium is unstable, due to the presence of a positive real eigenvalue, if $a_0 < 0$, i.e., $\bar{\mathcal{R}} > 1$ or, equivalently, $\bar{C}_U > \mathcal{C}_U^*$. When $\bar{\mathcal{R}} < 1$, or equivalently $\bar{C}_U < \mathcal{C}_U^*$, matrix $\mathbf{A}$ is Hurwitz, but the zero eigenvalue prevents us from drawing conclusions on the stability of the equilibria based on the system linearisation.

B. Asymptotic behaviour

Here, we show that the equilibrium subset

$$\mathcal{X}_{eq}^* = \{x \in \mathcal{X}_{eq} \colon 0 \le C_U \le \mathcal{C}_U^*\} \tag{12}$$

is the smallest set that is attractive in $\mathcal{X}$ (the distance from $\mathcal{X}_{eq}^*$ of all trajectories originated in $\mathcal{X}$ converges to zero as $t \to \infty$) and is Lyapunov stable (for all $\epsilon > 0$, there exists $\zeta > 0$ such that, if the distance of $x(t_0)$ from $\mathcal{X}_{eq}^*$ is smaller than ζ, then the distance of $x(t)$ from $\mathcal{X}_{eq}^*$ is smaller than ϵ for all $t \ge t_0$). Hence, $\mathcal{X}_{eq}^*$ is the smallest asymptotically stable equilibrium set, with domain of attraction $\mathcal{X}$.

All trajectories starting in $\mathcal{X}$ converge to a state in $\mathcal{X}_{eq}$.

Proposition 2 (Asymptotic behaviour)**.** *For system* (5)*, if* $x(t_0) \in \mathcal{X}$ *at some time* t_0*, then* $\lim_{t\to\infty} x(t) = x_{eq} \in \mathcal{X}_{eq}$*, with* $\lim_{t\to\infty} C_U(t) = C_\infty \in [0, C_U(t_0))$.

Proof. Being $\dot{C}_U(t) < 0 \ \forall t \ge t_0$ when $x(t_0) \in \mathcal{X}$, C_U is monotonically decreasing, hence $\lim_{t\to\infty} C_U(t) = C_\infty$ is a constant value in the interval $[0, C_U(t_0))$. As a consequence, $\lim_{t\to\infty} \dot{C}_U(t) = 0$ and, from (5a), $\lim_{t\to\infty} C_U(t) V_E(t) = 0$. Then $\lim_{t\to\infty} \dot{C}_L(t) = -\gamma C_L(t) \Rightarrow \lim_{t\to\infty} C_L(t) = 0 \Rightarrow \lim_{t\to\infty} \dot{C}_P(t) = -\delta C_P(t) \Rightarrow \lim_{t\to\infty} C_P(t) = 0 \Rightarrow \lim_{t\to\infty} \dot{V}_I(t) = -\eta V_I(t) \Rightarrow \lim_{t\to\infty} V_I(t) = 0 \Rightarrow \lim_{t\to\infty} \dot{V}_E(t) = -c V_E(t) \Rightarrow \lim_{t\to\infty} V_E(t) = 0$. □

We can show that $\mathcal{X}_{eq}^*$ is an attractive set, since $C_\infty \in [0, \mathcal{C}_U^*]$, and is actually the smallest.

Theorem 1 (Attractivity of $\mathcal{X}_{eq}^*$)**.** *For system* (5)*,* $\mathcal{X}_{eq}^*$ *in* (12) *is the smallest attractive equilibrium set in* $\mathcal{X}$.

Proof. To prove attractivity, we show that $C_\infty \in [0, \mathcal{C}_U^*]$. Summing the first three equations of system (5) yields $\dot{C}_U + \dot{C}_L + \dot{C}_P = -\delta C_P$. Rearranging (5d) gives

$$-\eta V_I = \dot{V}_I - p_r C_P = \dot{V}_I + \frac{p_r}{\delta}(\dot{C}_U + \dot{C}_L + \dot{C}_P),$$

while from (5e) we have

$$-c V_E = \dot{V}_E - \eta V_I = \dot{V}_E + \dot{V}_I + \frac{p_r}{\delta}(\dot{C}_U + \dot{C}_L + \dot{C}_P).$$

Dividing both sides of (5a) by C_U yields

$$\frac{\dot{C}_U}{C_U} = -\beta V_E = \frac{\beta}{c}(\dot{V}_E + \dot{V}_I) + \frac{p_r \beta}{\delta c}(\dot{C}_U + \dot{C}_L + \dot{C}_P).$$

Integrating and taking the limit for $t \to \infty$ of both sides, since $C_L(\infty) = C_P(\infty) = V_I(\infty) = V_E(\infty) = 0$, yields

$$\ln\left(\frac{C_U(\infty)}{C_{U,0}}\right) = \frac{p_r \beta}{\delta c} C_U(\infty) - \mathcal{R}_0 - \mathcal{Q}_0,$$

where $\mathcal{R}_0$, defined as in (9), and $\mathcal{Q}_0 = \frac{p_r \beta}{\delta c}(C_{L,0} + C_{P,0}) + \frac{\beta}{c}(V_{I,0} + V_{E,0})$ depend on the initial conditions. Taking the exponential of both sides and suitably rearranging leads to an equation of the form $a e^a = b$, where $a = -\frac{p_r \beta}{\delta c} C_U(\infty)$ and $b = -\mathcal{R}_0 e^{-(\mathcal{R}_0 + \mathcal{Q}_0)}$. A solution exists iff $b \ge -1/e$, which is the case here because $-\mathcal{R}_0 e^{-(\mathcal{R}_0+\mathcal{Q}_0)} \in [-1/e, 0]$, and is $a = W_0(b)$, where $W_0(\cdot)$ is the principal branch of the Lambert function, which maps $[-1/e, 0]$ into $[-1, 0]$. Hence,

$$C_\infty = C_U(\infty) = -\frac{\delta c}{p_r \beta} W_0(b) = -\mathcal{C}_U^* W_0(b) \in [0, \mathcal{C}_U^*].$$

Moreover, $\mathcal{X}_{eq}^*$ is the smallest attractive set in $\mathcal{X}$: from two different initial conditions, the system converges to two different equilibria in $\mathcal{X}_{eq}^*$, hence neither single states in $\mathcal{X}_{eq}^*$ nor subsets of $\mathcal{X}_{eq}^*$ are attractive in $\mathcal{X}$; for more details, see the proof of [9, Theorem 3.1] for a model of the form (6). □

We can also prove that $\mathcal{X}_{eq}^*$ is Lyapunov stable.

Theorem 2 (Lyapunov stability of $\mathcal{X}_{eq}^*$)**.** *For system* (5)*, the equilibrium set* $\mathcal{X}_{eq}^*$ *in* (12) *is Lyapunov stable.*

Proof. Given the generic equilibrium $\bar{x} = [\bar{C}_U \, 0 \, 0 \, 0 \, 0]$ with $\bar{C}_U \in [0, \mathcal{C}_U^*)$, we consider the candidate Lyapunov function

$$\mathcal{V}(x) = C_U - \bar{C}_U - \bar{C}_U \ln\left(\frac{C_U}{\bar{C}_U}\right) + C_L + C_P + \frac{\delta}{p_r}(V_I + V_E),$$

which is continuously differentiable, zero at the equilibrium and positive for all other $x \in \mathbb{R}^5_{\ge 0}$. The Lyapunov derivative is $\dot{\mathcal{V}}(x) = \nabla \mathcal{V}(x) \cdot \dot{x} = \begin{bmatrix} \left(1 - \frac{\bar{C}_U}{C_U}\right) & 1 & 1 & \frac{\delta}{p_r} & \frac{\delta}{p_r} \end{bmatrix} \begin{bmatrix} -\beta C_U V_E \\ \beta C_U V_E - \gamma C_L \\ \gamma C_L - \delta C_P \\ p_r C_P - \eta V_I \\ \eta V_I - c V_E \end{bmatrix}$ and

$$\dot{\mathcal{V}}(x) = V_E\left(\beta \bar{C}_U - \frac{\delta c}{p_r}\right) \le 0 \tag{13}$$

whenever $\bar{C}_U \le \mathcal{C}_U^*$. Hence, $\mathcal{V}$ is a Lyapunov function for system (5), proving stability of all equilibria in $\mathcal{X}_{eq}^*$. □

In view of Theorems 1 and 2, $\mathcal{X}_{eq}^*$ is asymptotically stable.

Theorem 3 (Asymptotic stability of $\mathcal{X}^*_{eq}$)**.** *For system* (5)*, $\mathcal{X}^*_{eq}$ in* (12) *is the smallest asymptotically stable equilibrium set, with domain of attraction $\mathcal{X}$.*

The domain of attraction cannot be the whole nonnegative orthant: all states with $C_U = 0$ or $V_E = 0$ are equilibria when $C_L = C_P = V_I = 0$.

The asymptotic number of uninfected cells enjoys properties akin to those proven in [9] for a system of the form (6). We state and prove the properties, visualised in Fig. 2.

Proposition 3 (Asymptotic value of C_U)**.** *For system* (5) *starting from the initial condition $[C_{U,0}\,0\,0\,0\,V_{E,0}] \in \mathcal{X}$, with $V_{E,0} > 0$ small enough, denoting by $C_\infty(C_{U,0})$ the asymptotic value of C_U with initial condition $C_{U,0}$, we have:*

- **(i)** $C_\infty(C_{U,0}) \to 0$ *if* $C_{U,0} \to \infty$ *or* $C_{U,0} \to 0$*;*
- **(ii)** $C_\infty(C_{U,0}) \to \mathcal{C}^*_U$ *if* $C_{U,0} \to \mathcal{C}^*_U$*;*
- **(iii)** $0 < C_\infty(C_1) < C_\infty(C_2) < \mathcal{C}^*_U$ *if* $C_1 < C_2 < \mathcal{C}^*_U$*;*
- **(iv)** $0 < C_\infty(C_2) < C_\infty(C_1) < \mathcal{C}^*_U$ *if* $\mathcal{C}^*_U < C_1 < C_2$*.*

Proof. From the proof of Theorem 1, we know that $C_\infty = -\mathcal{C}^*_U W_0\left(-\mathcal{R}_0 \mathrm{e}^{-(\mathcal{R}_0+\mathcal{Q}_0)}\right)$. Given an initial condition with $C_{L,0} = C_{P,0} = V_{I,0} = 0$ and $V_{E,0} \approx 0$, it is $\mathcal{Q}_0 \approx 0$ and thus $C_\infty \approx -\mathcal{C}^*_U W_0\left(-\mathcal{R}_0 \mathrm{e}^{-\mathcal{R}_0}\right)$. Then: **(i)** $W_0\left(-\mathcal{R}_0 \mathrm{e}^{-\mathcal{R}_0}\right) \to 0$ when $-\mathcal{R}_0 \mathrm{e}^{-\mathcal{R}_0} \to 0$, which happens if $\mathcal{R}_0 \to \infty$ ($C_{U,0} \to \infty$) or $\mathcal{R}_0 \to 0$ ($C_{U,0} \to 0$). **(ii)** When $C_{U,0} \to \mathcal{C}^*_U$, $\mathcal{R}_0 \to 1$. Thus, $C_\infty(C_{U,0}) \to -\mathcal{C}^*_U W_0(-e^{-1}) = \mathcal{C}^*_U$. **(iii)** $C_{U,0} < \mathcal{C}^*_U$ means $\mathcal{R}_0 < 1$. Since $-\mathcal{R}_0 \mathrm{e}^{-\mathcal{R}_0}$ is decreasing for $\mathcal{R}_0 \in (0,1)$, while $-W_0(\cdot)$ is decreasing for $(-e^{-1}, 0)$, the composed function is increasing: $0 < -W_0(-\mathcal{R}_1 \mathrm{e}^{-\mathcal{R}_1}) < -W_0(-\mathcal{R}_2 \mathrm{e}^{-\mathcal{R}_2})$ if $\mathcal{R}_2 > \mathcal{R}_1$ (i.e., $C_2 > C_1$). **(iv)** $C_{U,0} > \mathcal{C}^*_U$ means $\mathcal{R}_0 > 1$. Since $-\mathcal{R}_0 \mathrm{e}^{-\mathcal{R}_0}$ is increasing for $\mathcal{R}_0 \in (1, \infty)$, the composed function is decreasing: $0 < -W_0(-\mathcal{R}_2 \mathrm{e}^{-\mathcal{R}_2}) < -W_0(-\mathcal{R}_1 \mathrm{e}^{-\mathcal{R}_1})$ if $\mathcal{R}_2 > \mathcal{R}_1$ (i.e., $C_2 > C_1$). □

Remark 1 (Transient behaviour)**.** *The evolution of* (5) *is different from that of* (6)*, analysed e.g. in [9], for which, if $\mathcal{R}_0 \le 1$, $\dot{V}_E(t) \le 0$ for all $t > t_0$ when only $C_U(t_0)$ and $V_E(t_0)$ are non-zero. For some parameter choices, model* (5) *can yield an increase in V_E even when $\mathcal{R}_0 < 1$. Two typical behaviours of system* (5)*, shown in Fig. 3, correspond to monotonic healing ($\dot{V}_E(t) \le 0$) when $\mathcal{R}_0 < \bar{\mathcal{R}} < 1$ is small enough, and acute infection spreading otherwise. The different transient evolution suggests the importance of considering the full model to plan treatment, whenever the dynamics of C_L and V_I cannot be safely neglected.*

IV. Optimal Treatment with Antiviral Drugs

We demonstrate how our novel model could be used to support optimal mpox treatment. Interest in mpox has only very recently arisen and therefore the available data are still scarce. Our model parameters are thus not identified from time series, due to the lack of specific clinical data, but inferred from the literature, also on the closely related Vaccinia virus [24]. Here, we exemplify the general methodology and the insight that our novel model could provide within an optimal control framework for therapy design,

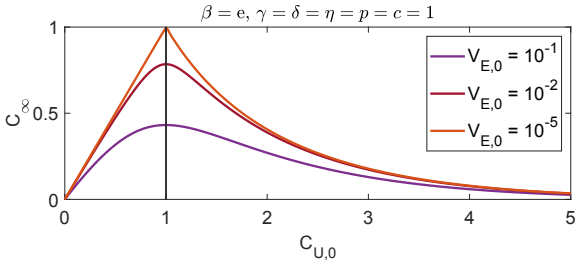

Fig. 2: Asymptotic value C_∞ of C_U as a function of the initial condition $C_{U,0}$, when $\beta = e$ and all other parameters are set to 1, resulting in $\mathcal{C}^*_U = 1$. All the statements in Proposition 3 hold for $V_{E,0} = 10^{-5}$. As the initial amount of external virus $V_{E,0}$ is increased, $C_\infty(\mathcal{C}^*_U) < \mathcal{C}^*_U$, but all statements except for **(ii)** still hold.

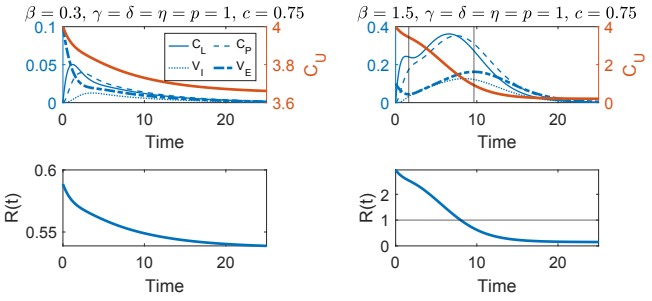

Fig. 3: Time evolution of the state variables in (5) and of $\mathcal{R}(t)$. Left: $\mathcal{R}_0 < \bar{\mathcal{R}} < 1$; V_E decreases monotonically. Right: $\mathcal{R}_0 > 1$; V_E first decreases, reaches a minimum, then grows up to a maximum (and keeps growing while $\bar{\mathcal{R}} < \mathcal{R}(t) < 1$) before finally decreasing to zero.

once the most appropriate parameter values for the specific clinical case have been chosen. The resulting optimal therapy depends on the parameter values, which are subject to large uncertainties and variability across patients. Even though all the model parameters are specific for each patient, given the typical infection and treatment duration of about 14 days [5], [30], the time required for data collection on the single patient would lead to late therapeutic interventions; a possible practical approach towards personalised treatment is to plan specific therapies for different patient categories, taking into account e.g. age, sex, weight, specific risk factors.

We assume that the antiviral drugs *cidofovir* (inhibiting intracellular virus production, thus reducing p) and *tecovirimat* (inhibiting intracellular virus excretion, thus reducing η) can be infused daily (for 12 hours) through inputs u_1 and u_2 respectively. Each drug administration cannot exceed a maximum tolerated dose. The drug concentrations $D_i(t)$, $i = 1, 2$, in the body exhibit first-order decay, as is common in pharmacokinetic modelling:

$$\dot{D}_i(t) = u_i(t) - k_i D_i(t), \qquad i = 1, 2.$$

Each drug inhibits its target process through a Michaelis-Menten function of D_i, with half-inhibitory concentration h_i [31]. Hence, the drug-dependent rate constants are:

$$\hat{p}(D_1) = \frac{h_1}{h_1 + D_1} p \quad \text{and} \quad \hat{\eta}(D_2) = \frac{h_2}{h_2 + D_2} \eta. \tag{14}$$

Our goal is to minimise the viral load V_E over a finite horizon, both throughout the dynamic evolution (with an integral cost) and at the final time (with a terminal cost),

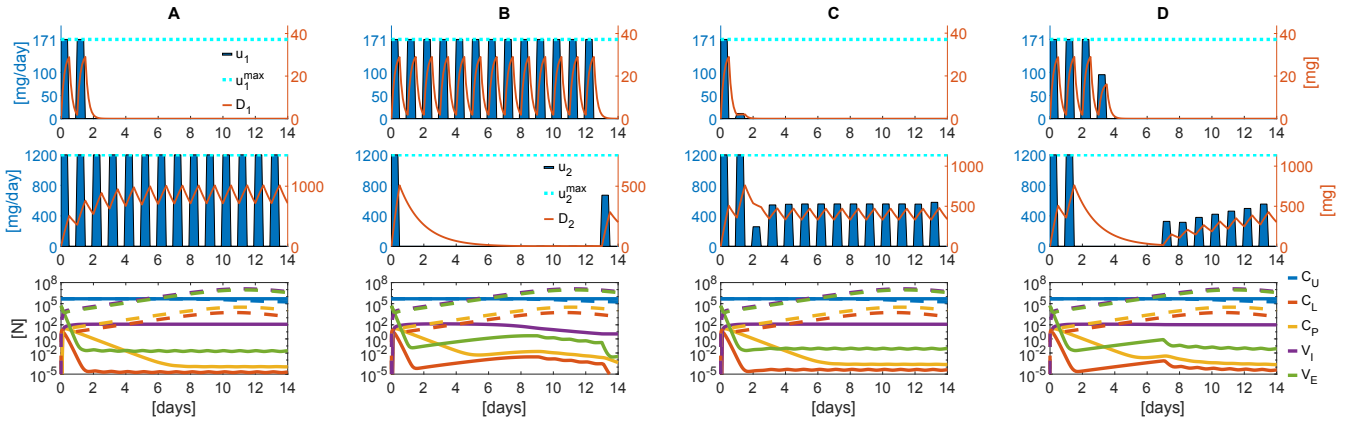

Fig. 4: Optimal drug administration as a solution to the optimal control problem (16) with cost functional (15). The model parameters are chosen based on the literature on the similar, well studied Vaccinia virus [24]: $\gamma = 12$ [days^{-1}], since the latent period typically lasts 2 hours [25]; $\delta = 2$ [days^{-1}] as a worst-case choice, since productive cell lifetime is at least 5-7 hours [26]; $p = 5,000$ [days^{-1}], since at least 5,000 internal virus copies have been detected per cell one day after infection [27]; $\eta = 10$ [days^{-1}], since shedding occurs about 2-3 hours after production [28]; $c = \log(2) \cdot 144/7$ [days^{-1}], since the virus half-life is about 70 minutes in blood [29]; $\beta = 2.4 \cdot 10^{-8}$ [days^{-1}] to result in a typical infection duration of 6-13 days [5]. The drug parameters are inferred from the recent work [8]: $k_1 = \log(2) \cdot 8$ [days^{-1}] and $k_2 = \log 2$ [days^{-1}], since the half-lives of *cidofovir* and *tecovirimat* are about 4 hours and 24 hours; $h_1 = 56$ [mg] and $h_2 = 0.19$ [mg]; $u_1^{max} = 171$ [mg day^{-1}] and $u_2^{max} = 1200$ [mg day^{-1}], assuming constant infusion for 12 hours followed by 12 hours without infusion. The initial conditions are set as $C_{U,0} = 5 \cdot 10^5$ [N], $C_{L,0} = C_{P,0} = V_{I,0} = 0$ [N], $V_{E,0} = 5 \cdot 10^4$ [N], $D_{1,0} = D_{2,0} = 0$ [mg]. As for the cost weights, $\alpha_1 = 0.01$ and $\alpha_2 = 0.001$ in all cases, while the scenarios shown in the four columns differ for the choice of w_1, w_2, w_3. A: $w_1 = 100$, $w_2 = 1$, $w_3 = 0$; B: $w_1 = 100$, $w_2 = 1$, $w_3 = 10$; C: $w_1 = 10$, $w_2 = 1$, $w_3 = 0$; D: $w_1 = 10$, $w_2 = 1$, $w_3 = 0.1$. The figure shows the time evolution of: u_1 and D_1, in the first row; u_2 and D_2, in the second row; the state variables of the infection system, in logarithmic scale, in the third row, where solid lines represent the evolution of the controlled system, while dashed lines represent the evolution of system (5), with the same parameters, in the absence of pharmaceutical treatment: $u_1(t) = u_2(t) = 0$.

and possibly also V_I throughout the horizon. This maximises the amount of surviving healthy cells C_U. We also wish to minimise the side effects caused by the two drugs [32], [33]. With weights $w_1, w_2, w_3, \alpha_1, \alpha_2 \geq 0$ and cost functional

$$F = \int_0^T \big(w_1 V_E(t) + \alpha_1 D_1(t) + \alpha_2 D_2(t) + w_3 V_I(t)\big)dt + w_2 V_E(T), \tag{15}$$

the optimal control problem can be formulated as:

$$\min_{u_1(t), u_2(t)} F(V_E, V_I, D_1, D_2) \tag{16a}$$

$$\dot{C}_U = -\beta C_U V_E \tag{16b}$$

$$\dot{C}_L = \beta C_U V_E - \gamma C_L \tag{16c}$$

$$\dot{C}_P = \gamma C_L - \delta C_P \tag{16d}$$

$$\dot{V}_I = \hat{p}(D_1) C_P - \hat{\eta}(D_2) V_I - \frac{\hat{p}(D_1)}{\hat{\eta}(D_2)} \left[1 - \mathrm{e}^{-\frac{\hat{\eta}(D_2)}{\delta}}\right] \delta C_P \tag{16e}$$

$$\dot{V}_E = \hat{\eta}(D_2) V_I - c V_E \tag{16f}$$

$$\dot{D}_i = u_i(t) - k_i D_i, \quad i = 1, 2 \tag{16g}$$

$$0 \leq u_i \leq u_i^{\max}, \quad i = 1, 2 \tag{16h}$$

where the input is piecewise constant: $u_i(t) = u_{i,j}$ for $t \in [t_j, t_{j+1}]$, with $j = 1, \ldots, N-1$, $t_1 = 0$, $t_N = T = 14$ days and $t_{j+1} - t_j = 12$ hours $\forall j$; and it is $u_{i,j} = 0$ for j even.

We numerically solve the optimal control problem with a multiple shooting method using CasADi [34] through its MATLAB interface. We assume a treatment period of 14 days. The chosen parameter values are discussed in the caption of Fig. 4, which compares the effects of the optimal treatment schedules obtained with different choices of the cost weights.

The four scenarios illustrate the type of conceptual insight that we can expect from embedding our model within an optimal control approach. In the clinical practice, *tecovirimat* is preferred over *cidofovir* [5], [31], because it has a stronger efficacy for the same dose (in fact, we set $h_1 \gg h_2$) and milder side effects (in fact, we choose the cost weights as $\alpha_2 = 0.001 < \alpha_1 = 0.01$). Even though all the advantages of *tecovirimat* are reflected in our chosen parameters, our numerical results show that the optimal choice is not to administer *tecovirimat* only (as is typically done in practice), but to use (small) doses of *cidofovir* in synergy with it.

To allow a complete comparison, not only between the considered treatment scenarios, but also between the treated and untreated evolution, all the bottom panels of Fig. 4 also report, with dashed lines, the dynamic evolution of the system with the same parameters, but without any treatment ($u_1 = u_2 = 0$). Without treatment, in 15 days C_U would be reduced from its initial value of $5 \cdot 10^5$ to $5 \cdot 10^4$ (while the viral load values would have a peak around 10^7), leading to tissue necrosis and to the patient's death. In Fig. 4A ($w_1 = 100$, $w_2 = 1$, $w_3 = 0$), both controls are saturated, although *cidofovir* (u_1) is only given for the first two days, while *tecovirimat* (u_2) for the whole therapy horizon; however, even though V_E is brought below one, V_I decreases very slowly. When a fast reduction of the amount of intracellular virus is an important objective, as in Fig. 4B ($w_1 = 100$, $w_2 = 1$, $w_3 = 10$), an even stronger use of *cidofovir* becomes necessary. Conversely, in Fig. 4C ($w_1 = 10$, $w_2 = 1$, $w_3 = 0$), *cidofovir* (u_1) is only given for the first day at the maximum dose and for the second day at a small dose, while *tecovirimat* (u_2) is given for the whole therapy horizon, at the maximum dose for the first two days and at smaller doses afterwards. In Fig. 4D ($w_1 = 10$, $w_2 = 1$, $w_3 = 0.1$), a slightly faster reduction of V_I is required (barely noticeable in logarithmic scale) and is obtained with higher doses of *cidofovir* and smaller doses of *tecovirimat*.

It is worth stressing that, to successfully reach the treat-

ment goal, it is not necessary to drive V_E and V_I to zero: once the viral load goes below a safe threshold, the patient's immune system will take care of it and suppress the infection.

V. Concluding Discussion

We have proposed a new model of in-host virus infection dynamics that explicitly captures internal virus production and shedding, to account for the respective effects of the antiviral drugs *cidofovir* and *tecovirimat*, candidates in the treatment of mpox. The classic target-cell limited model is recovered from the proposed model as a quasi-steady-state approximation; we have shown that our model shares many features with the target-cell limited model, such as equilibria and asymptotic behaviours, but can have different transient behaviours. With model parameters taken from the medical literature, we have showcased the general methodology to formulate and solve an optimal treatment control problem, illustrating how our model can be used to support the optimal scheduling of antiviral drug therapies. Future work includes quantitative model validation and parameterisation based on infection time-series data from *in vitro* experiments and/or patients suffering from mpox infection, so as to inform real therapies through optimal control approaches with tailored parameter values. Since previous studies have effectively used the target-cell limited model with constant coefficients to fit real viral infection data (e.g. for HIV, West Nile virus and Influenza [35]–[37]), we expect that our proposed model, which is more detailed and thus more flexible, will be able to match real data even with constant coefficients.

References

[1] J. P. Thornhill, *et al.*, "Monkeypox virus infection in humans across 16 countries: April–June 2022," *New Engl. J. Med.*, vol. 387, no. 8, pp. 679–691, 2022.

[2] Q. Zheng, C. Bao, P. Li, A. C. de Vries, G. Giordano, and Q. Pan, "Projecting the impact of testing and vaccination on the transmission dynamics of the 2022 monkeypox outbreak in the USA," *J. Travel Med.*, vol. 29, no. 8, p. taac101, 2022.

[3] M. E. DeWitt, *et al.*, "Global monkeypox case hospitalisation rates: A rapid systematic review and meta-analysis," *eClinicalMedicine*, vol. 54, p. 101710, 2022.

[4] G. Andrei and R. Snoeck, "Cidofovir activity against poxvirus infections," *Viruses*, vol. 2, no. 12, pp. 2803–2830, 2010.

[5] A. Mondi, *et al.*, "Clinical experience with use of oral tecovirimat or intravenous cidofovir for the treatment of monkeypox in an Italian reference hospital," *J. Infect.*, vol. 86, no. 1, pp. 66–117, 2023.

[6] G. Yang, *et al.*, "An orally bioavailable antipoxvirus compound (ST-246) inhibits extracellular virus formation and protects mice from lethal orthopoxvirus challenge," *J. Virol.*, vol. 79, no. 20, pp. 13 139–13 149, 2005.

[7] A. Sherwat, J. T. Brooks, D. Birnkrant, and P. Kim, "Tecovirimat and the treatment of monkeypox: Past, present, and future considerations," *New Engl. J. Med.*, vol. 387, no. 7, pp. 579–581, 2022.

[8] E. A. Siegrist and J. Sassine, "Antivirals with activity against mpox: A clinically oriented review," *Clin. Infect. Dis.*, vol. 76, no. 1, pp. 155–164, 2023.

[9] P. Abuin, A. Anderson, A. Ferramosca, E. A. Hernandez-Vargas, and A. H. Gonzalez, "Characterization of SARS-CoV-2 dynamics in the host," *Annu. Rev. Control*, vol. 50, pp. 457–468, 2020.

[10] ——, "Dynamical characterization of antiviral effects in COVID-19," *Annu. Rev. Control*, vol. 52, pp. 587–601, 2021.

[11] A. Dutta, "Optimizing antiviral therapy for COVID-19 with learned pathogenic model," *Sci. Rep.*, vol. 12, no. 1, p. 6873, 2022.

[12] S. Ahmed, S. Rahman, and M. Kamrujjaman, "Optimal treatment strategies to control acute HIV infection," *Infect. Dis. Model.*, vol. 6, pp. 1202–1219, 2021.

[13] E. Hernandez-Vargas, P. Colaneri, R. Middleton, and F. Blanchini, "Discrete-time control for switched positive systems with application to mitigating viral escape," *Int. J. Robust Nonlin. Control*, vol. 21, no. 10, pp. 1093–1111, 2011.

[14] E. A. Hernandez-Vargas, P. Colaneri, and R. H. Middleton, "Optimal therapy scheduling for a simplified HIV infection model," *Automatica*, vol. 49, no. 9, pp. 2874–2880, 2013.

[15] ——, "Switching strategies to mitigate HIV mutation," *IEEE Trans. Control Syst. Technol.*, vol. 22, no. 4, pp. 1623–1628, 2014.

[16] A. N. Phillips, "Reduction of HIV concentration during acute infection: Independence from a specific immune response," *Science*, vol. 271, no. 5248, pp. 497–499, 1996.

[17] A. Handel, N. L. La Gruta, and P. G. Thomas, "Simulation modelling for immunologists," *Nat. Rev. Immunol.*, vol. 20, no. 3, pp. 186–195, 2020.

[18] A. Timm and J. Yin, "Kinetics of virus production from single cells," *Virology*, vol. 424, no. 1, pp. 11–17, 2012.

[19] K. L. Roberts and G. L. Smith, "Vaccinia virus morphogenesis and dissemination," *Trends Microbiol.*, vol. 16, no. 10, pp. 472–479, Oct. 2008.

[20] D. Richeson and J. Wiseman, "A fixed point theorem for bounded dynamical systems," *Ill. J. Math.*, vol. 46, no. 2, pp. 491–495, 2002.

[21] R. Srzednicki, "On rest points of dynamical systems," *Fundam. Math.*, vol. 126, no. 1, pp. 69–81, 1985.

[22] O. Diekmann, J. Heesterbeek, and J. Metz, "On the definition and the computation of the basic reproduction ratio R_0 in models for infectious diseases in heterogeneous populations," *J. Math. Biol.*, vol. 28, no. 4, 1990.

[23] P. van den Driessche and J. Watmough, "Reproduction numbers and sub-threshold endemic equilibria for compartmental models of disease transmission," *Math. Biosci.*, vol. 180, no. 1-2, pp. 29–48, 2002.

[24] Q. Gong, C. Wang, X. Chuai, and S. Chiu, "Monkeypox virus: a re-emergent threat to humans," *Virol. Sin.*, vol. 37, no. 4, pp. 477–482, Aug. 2022.

[25] M. D. Greseth and P. Traktman, "The life cycle of the Vaccinia virus genome," *Annu. Rev. Virology*, vol. 9, no. 1, pp. 239–259, Sept. 2022.

[26] A. Alkhalil, R. Hammamieh, J. Hardick, M. A. Ichou, M. Jett, and S. Ibrahim, "Gene expression profiling of monkeypox virus-infected cells reveals novel interfaces for host-virus interactions," *Virol. J.*, vol. 7, no. 1, p. 173, Dec. 2010.

[27] W. K. Joklik and Y. Becker, "The replication and coating of Vaccinia DNA," *J. Molec. Biol.*, vol. 10, no. 3, pp. 452–474, Dec. 1964.

[28] D. W. Grosenbach and D. E. Hruby, "Analysis of a Vaccinia virus mutant expressing a nonpalmitylated form of p37, a mediator of virion envelopment," *J. Virol.*, vol. 72, no. 6, pp. 5108–5120, June 1998.

[29] H. J. Zeh, *et al.*, "First-in-man study of western reserve strain oncolytic vaccinia virus: safety, systemic spread, and antitumor activity," *Mol. Ther.*, vol. 23, no. 1, pp. 202–214, Jan. 2015.

[30] F. Dammann, M. Raja, and J. F. Camargo, "Progression of human monkeypox infection despite tecovirimat in an immunocompromised adult," *Transpl- Infect. Dis.*, vol. 25, no. 1, Feb. 2023.

[31] G. Frenois-Veyrat, *et al.*, "Tecovirimat is effective against human monkeypox virus in vitro at nanomolar concentrations," *Nat. Microbiol.*, vol. 7, no. 12, pp. 1951–1955, Nov. 2022.

[32] G. Giordano, A. Rantzer, and V. D. Jonsson, "A convex optimization approach to cancer treatment to address tumor heterogeneity and imperfect drug penetration in physiological compartments," in *IEEE 55th Conf. Dec. Control (CDC)*, 2016, pp. 2494–2500.

[33] C. A. Devia and G. Giordano, "Optimal duration and planning of switching treatments taking drug toxicity into account: a convex optimisation approach," in *IEEE 58th Conf. Dec. Control (CDC)*, 2019, pp. 5674–5679.

[34] J. A. E. Andersson, J. Gillis, G. Horn, J. B. Rawlings, and M. Diehl, "CasADi: A software framework for nonlinear optimization and optimal control," *Math. Program. Comput.*, 2018.

[35] S. M. Ciupe and J. M. Heffernan, "In-host modeling," *Infect. Dis. Model.*, vol. 2, no. 2, pp. 188–202, 2017.

[36] S. Banerjee, J. Guedj, R. M. Ribeiro, M. Moses, and A. S. Perelson, "Estimating biologically relevant parameters under uncertainty for experimental within-host murine West Nile virus infection," *J. Royal Soc. Interface*, vol. 13, no. 117, p. 20160130, Apr. 2016.

[37] R. Sachak-Patwa, E. I. Lafferty, C. J. Schmit, R. N. Thompson, and H. M. Byrne, "A target-cell limited model can reproduce influenza infection dynamics in hosts with differing immune responses," *J. Theor. Biol.*, vol. 567, p. 111491, June 2023.